



AFRL-RX-WP-TP-2010-4052

**SYMMETRY-BASED AUTOMATED EXTRACTION OF
MICROSTRUCTURAL FEATURES: APPLICATION TO
DENDRITIC CORES IN SINGLE-CRYSTAL Ni-BASED
SUPERALLOYS (POSTPRINT)**

M.A. Groeber, J.P. Simmons, A.H. Rosenberger, and C. Woodward

Metals Branch
Metals, Ceramics & NDE Division

M.A. Tschopp
Mississippi State University

R. Fahringer
University of Dayton

JANUARY 2010

Approved for public release; distribution unlimited.

See additional restrictions described on inside pages

STINFO COPY

© 2009 Acta Materialia Inc.

**AIR FORCE RESEARCH LABORATORY
MATERIALS AND MANUFACTURING DIRECTORATE
WRIGHT-PATTERSON AIR FORCE BASE, OH 45433-7750
AIR FORCE MATERIEL COMMAND
UNITED STATES AIR FORCE**

REPORT DOCUMENTATION PAGE

*Form Approved
OMB No. 0704-0188*

The public reporting burden for this collection of information is estimated to average 1 hour per response, including the time for reviewing instructions, searching existing data sources, gathering and maintaining the data needed, and completing and reviewing the collection of information. Send comments regarding this burden estimate or any other aspect of this collection of information, including suggestions for reducing this burden, to Department of Defense, Washington Headquarters Services, Directorate for Information Operations and Reports (0704-0188), 1215 Jefferson Davis Highway, Suite 1204, Arlington, VA 22202-4302. Respondents should be aware that notwithstanding any other provision of law, no person shall be subject to any penalty for failing to comply with a collection of information if it does not display a currently valid OMB control number. **PLEASE DO NOT RETURN YOUR FORM TO THE ABOVE ADDRESS.**

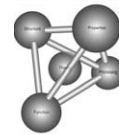
1. REPORT DATE (DD-MM-YY) January 2010			2. REPORT TYPE Journal Article Postprint		3. DATES COVERED (From - To) 01 January 2010 – 31 January 2010	
4. TITLE AND SUBTITLE SYMMETRY-BASED AUTOMATED EXTRACTION OF MICROSTRUCTURAL FEATURES: APPLICATION TO DENDRITIC CORES IN SINGLE-CRYSTAL Ni-BASED SUPERALLOYS (POSTPRINT)			5a. CONTRACT NUMBER FA8650-04-C-5200 5b. GRANT NUMBER 5c. PROGRAM ELEMENT NUMBER 62102F			
6. AUTHOR(S) M.A. Groeber, J.P. Simmons, A.H. Rosenberger, and C. Woodward (AFRL/RXLM) M.A. Tschopp (Mississippi State University) R. Fahringer (University of Dayton)			5d. PROJECT NUMBER 4347 5e. TASK NUMBER RG 5f. WORK UNIT NUMBER M02R3000			
7. PERFORMING ORGANIZATION NAME(S) AND ADDRESS(ES) Metals Branch (AFRL/RXLM) Metals, Ceramics & NDE Division Materials and Manufacturing Directorate Wright-Patterson Air Force Base, OH 45433-7750 Air Force Materiel Command, United States Air Force			Mississippi State University Center for Advanced Vehicular Systems Starkville, MS 39762 University of Dayton Dayton, OH 45431			
9. SPONSORING/MONITORING AGENCY NAME(S) AND ADDRESS(ES) Air Force Research Laboratory Materials and Manufacturing Directorate Wright-Patterson Air Force Base, OH 45433-7750 Air Force Materiel Command United States Air Force			8. PERFORMING ORGANIZATION REPORT NUMBER 10. SPONSORING/MONITORING AGENCY ACRONYM(S) AFRL/RXLMN 11. SPONSORING/MONITORING AGENCY REPORT NUMBER(S) AFRL-RX-WP-TP-2010-4052			
12. DISTRIBUTION/AVAILABILITY STATEMENT Approved for public release; distribution unlimited.						
13. SUPPLEMENTARY NOTES Journal article published in <i>Scripta Materialia</i> , Vol. 62 (2010). PAO Case Number: 88ABW-2009-4447; Clearance Date: 21 Oct 2009. © 2009 Acta Materialia Inc.. The U.S. Government is joint author of this work and has the right to use, modify, reproduce, release, perform, display, or disclose the work. Paper contains color.						
14. ABSTRACT Serial sectioning methods continue to produce a wealth of image data for quantifying the three-dimensional nature of material microstructures. Here, we discuss a computational methodology for automated detection and 3D characterization of dendrite cores from images taken from slices of a production turbine blade made of a heat-treated single crystal Ni-based superalloy. The dendrite core locations are detected using an automated segmentation technique that incorporates information over multiple length scales and exploits the four-fold symmetry of the dendrites when viewed down the <001> growth direction. Additional rules that take advantage of the continuity of the dendrites from slice to slice help to exclude segmentation artifacts and improve dendrite core segmentation. The significance of this technique is that it can be extended to include any symmetry features such as mirror planes, improper rotations, or color symmetry, by using suitable matrix representations of these operations. For simplicity, only the four-fold rotation is included in this work.						
15. SUBJECT TERMS single crystal, nickel-based superalloy, characterization, dendrite core, feature extraction, image processing						
16. SECURITY CLASSIFICATION OF: a. REPORT Unclassified b. ABSTRACT Unclassified c. THIS PAGE Unclassified			17. LIMITATION OF ABSTRACT: SAR	18. NUMBER OF PAGES 10	19a. NAME OF RESPONSIBLE PERSON (Monitor) Reji John 19b. TELEPHONE NUMBER (Include Area Code) N/A	



Available online at www.sciencedirect.com



Scripta Materialia 62 (2010) 357–360



Scripta MATERIALIA

www.elsevier.com/locate/scriptamat

Symmetry-based automated extraction of microstructural features: Application to dendritic cores in single-crystal Ni-based superalloys

M.A. Tschopp,^{a,b,*} M.A. Groeber,^a R. Fahringer,^c J.P. Simmons,^a
A.H. Rosenberger^a and C. Woodward^a

^aAir Force Research Laboratory, Materials and Manufacturing Directorate, AFRL/RX Wright Patterson AFB, OH 45433, USA

^bCenter for Advanced Vehicular Systems, Mississippi State University, Starkville, MS 39762, USA

^cUniversity of Dayton, Dayton, OH 45431, USA

Received 10 September 2009; revised 26 October 2009; accepted 27 October 2009

Available online 30 October 2009

By exploiting the (prior) knowledge that certain microstructural features should, on average, have a certain symmetry, it was possible to develop an automated technique for identifying their locations within a complex microstructure. Subsequently, this technique is applied to a single-crystal Ni-based superalloy to identify dendrite core locations by using their fourfold symmetry as viewed along the $\langle 1\ 0\ 0 \rangle$ growth direction. Results of such a technique show good agreement with time-intensive manual identification of dendrite core locations.

© 2009 Acta Materialia Inc. Published by Elsevier Ltd. All rights reserved.

Keywords: Nickel alloys; Image analysis; 2-D quantitative analysis; Superalloy; Microstructure

Serial sectioning techniques and increasing image resolution is leading to an abundance of image data for characterizing the three-dimensional (3-D) structure of material microstructures [1–7]. As advances in these areas continue, there is an increasing need to process this information in an automated manner to extract useful microstructural statistics [8–10]. Interestingly, in materials science applications, symmetry often plays a role in the development of microstructure (especially in crystallography), yet symmetry is seldom used for image-processing techniques.

The present paper discusses an automated image processing technique for extracting symmetric features in microstructural images. Subsequently, this technique is applied to a single crystal Ni-based superalloy to identify dendrite core locations by using their fourfold symmetry as viewed along the $\langle 1\ 0\ 0 \rangle$ growth direction. Application to this particular problem is motivated by the large amount of time required to manually identify dendrite cores on each serial slice. Typical data sets can contain 50 or more serial slices with at least 250 dendrite cores per slice, so the time required to manually

identify these features is substantial. As the number of slices and dendrite cores increase, automated approaches for extracting the dendrite core locations is clearly required. The significance of this technique is that it can be extended to include any symmetry features such as mirror planes, improper rotations or color symmetry, by using suitable matrix representations of these operations. For simplicity, only the fourfold rotation is included in this work.

Figure 1 shows an etched optical image montage for a serial slice perpendicular to the nominal growth direction of a single crystal Ni-based superalloy (PWA 1484) turbine blade, which was fillet cut through the interior passage. The green (small) box is an image showing a single dendrite as viewed from the $\langle 1\ 0\ 0 \rangle$ growth direction and is used for describing the algorithm in Figure 2. The blue (intermediate) box is an image of a group of dendrites along with eutectic particles (bright particles within the interdendritic area), which is used to assess the symmetry-based technique (Fig. 3). Finally, the red (large) box delineates a 6 mm × 6 mm subset of the turbine blade that is subsequently used to test the technique on a microstructural area with a large number of features that can bias the calculation (i.e. both the mount material and eutectic particles).

Conventional image processing uses only the intensity information in the image, which is conventionally

* Corresponding author. Address: Center for Advanced Vehicular Systems, Mississippi State University, MS 39762, USA. Tel.: +1 662 325 5580; e-mail: mtschopp@cavs.msstate.edu

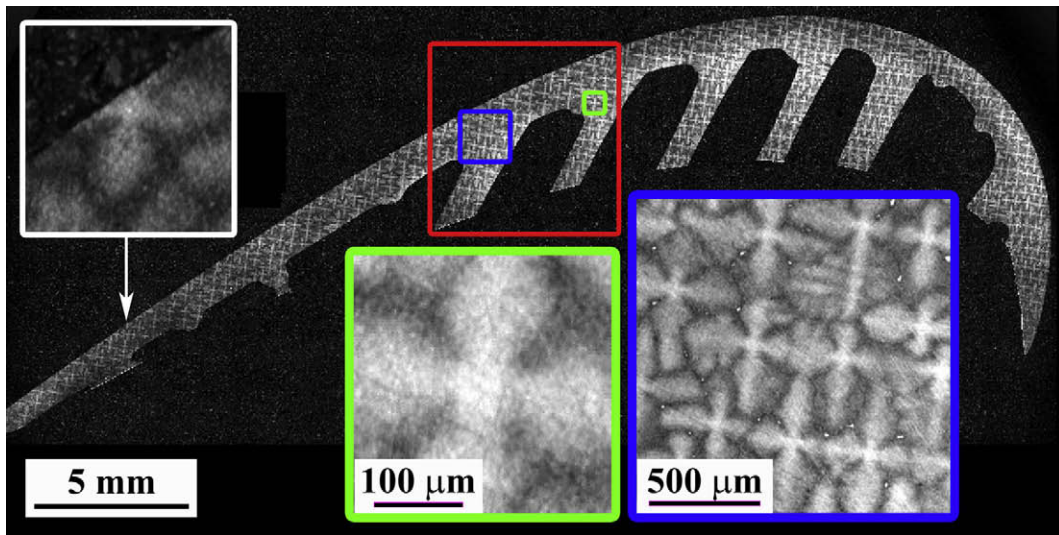


Figure 1. This image montage shows the microstructure of a cross-section of a single-crystal Ni-based superalloy turbine blade. The red, blue and green boxes highlight microstructural areas used for the symmetry-based technique. (For interpretation of the references to color in this figure legend, the reader is referred to the web version of this paper.)

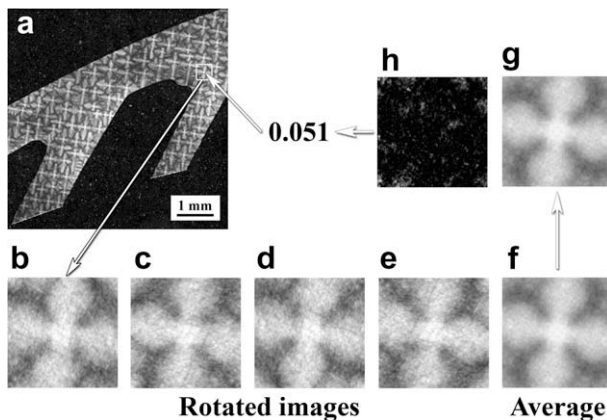


Figure 2. This schematic shows how a single pixel within the image is processed using the fourfold symmetry filter. (a) $300 \mu\text{m} \times 300 \mu\text{m}$ local image (b) surrounding a single pixel within (a) is chosen and rotated in 90° increments to produce (c–e). Image (f) is the average of the four rotated images and (g) is the corrected average for the mount material and eutectic particles (not required here). Image (h) shows the deviation between image (g) and image (b). The inverse of the sum of the values in image (h) is the fourfold symmetry parameter for the starting pixel.

known as “observation information”. This work builds on conventional methods by including the “prior information” that the cores should, on average, have fourfold symmetry, when viewed along the $\langle 1\ 0\ 0 \rangle$ growth direction. This is shown in **Figure 1**. The observation information would be the differences in intensity and textures for the different constituents of the image: the mount material, the dendrites, the eutectic particles and the interdendritic region. Combining this observation information with the prior information of the symmetry allows automatic identification of the cores.

By calculating a quantitative symmetry parameter for each pixel in an intensity image, those pixels in local neighborhoods with a high fourfold symmetry parameter can be detected using a simple threshold. **Figure 2**

shows a schematic of how the symmetry parameter is evaluated for a single pixel.

The red (large) image from **Figure 1** is shown in **Figure 2a**. The fourfold symmetry parameter for a single pixel within this image is calculated as follows:

- (1) A single pixel within **Figure 2a** is chosen to calculate the fourfold symmetry parameter. Then, a local neighborhood around the pixel is identified for a particular length scale (e.g. $300 \mu\text{m} \times 300 \mu\text{m}$ in **Fig. 2**) and the associated intensity image of this neighborhood is used for the fourfold symmetry filter (**Fig. 2b**).
- (2) The intensity image (**Fig. 2b**) is subsequently rotated by 90° three times to produce the images shown in **Fig. 2c–e**.
- (3) A local average intensity image (**Fig. 2f**) is calculated from the four rotated images in **Figure 2b–e**. When there are features within the local neighborhood that should not be taken into account for the fourfold symmetry parameter, the average intensity image may need to be corrected. **Figure 2g** is the result after accounting for these features (no effect in this example).
- (4) **Figure 2h** shows an image of the deviation at every pixel between the intensity values in **Figure 2 g** and **b**, where black pixels indicate a relatively low deviation. The l^2 -norm (square root of the sum of the squares of the pixels) is inverted to calculate the symmetry parameter of the local neighborhood for the single starting pixel.

To test the applicability of the fourfold symmetry filter to extracting dendrite core locations, the $1.4 \text{ mm} \times 1.4 \text{ mm}$ blue (intermediate) image was selected from the serial slice. Three different neighborhood sizes were used to investigate the influence of neighborhood size on the results: 100, 200 and $300 \mu\text{m}$. **Figure 3** shows the resulting images for the fourfold symmetry

filter using neighborhood sizes of 100 μm (a), 200 μm (b) and 300 μm (c). Visual comparison of the dendrite core locations in the original image (Fig. 1, blue) with the fourfold filtered images shows that the intensity is high in the dendrite core locations. However, the intensity is also often high in the secondary arms and sometimes in the interdendritic area, so a simple threshold at any length scale may be inadequate for segmenting the dendrite core locations from these filtered images. The original intensity information can also be useful for detecting the correct symmetric features (e.g. distinguishing fourfold symmetric dendritic regions from fourfold symmetric interdendritic regions). Also, notice that the eutectic particles in Figure 3a–c are shown in black. This does not reflect an absence of fourfold symmetry in these particles; rather, the eutectic particles were previously segmented and are accounted for in the fourfold symmetry filter so they do not affect the extraction of the dendrite core locations.

The technique was made more robust by segmenting the dendrite core locations with a vector-based segmentation approach using the fourfold symmetry parameters. In this manner, each pixel within the original image has a vector associated with it that reflects information from multiple length scales. For example, in this case, the fourfold symmetry parameters for local neighborhoods of 100, 150, 200, 250 and 300 μm were used to construct a vector-based image to help segment the dendrite cores. Then, the dimensionality of this vector-based image is reduced by taking the L^2 -norm of the vector within each pixel and multiplying by the original intensity image (to further reduce peaks in secondary/tertiary dendrite arms and interdendritic areas). Again, the intensity information of the original image is used to differentiate fourfold symmetry in the dendrite cores from that in the interdendritic regions. Additionally, weighting the fourfold symmetry parameter at different length scales with the corresponding standard deviation of the local neighborhood intensities is important for smaller length scales where high fourfold symmetry parameters may reflect that the homogeneity of intensities within a local neighborhood rather than the actual fourfold symmetry (e.g. the local region lies entirely within a dendrite arm). Figure 3d shows the resulting image after applying a Gaussian smoothing operation

and a morphological top hat filter. Notice that the image contrast has vastly increased over the images at the various length scales (Fig. 3a–c). Also, the dendrite cores appear much brighter than the dendrite arms, which display twofold symmetry.

The resulting image from the multiscale fourfold symmetry filter can now be segmented to extract the dendrite core locations. Prior to this point, the fourfold symmetry filters can operate in an automated fashion requiring no user intervention. While various automated segmentation methods exist (e.g. [8,9]), this image is easily segmented using a user-defined threshold parameter. In this image, the range of user-defined intensity thresholds that correctly identified all dendrite core locations was quite large (range of 142–204 when this image was rescaled to an 8-bit image). Figure 3e superimposes the segmented dendrite core locations (in red) obtained using a threshold parameter of 145 onto the original intensity image. This technique identified all the dendrite cores while only requiring the manual manipulation of a single parameter (the threshold parameter).

Extending the fourfold symmetry filter to the large image in Figure 1 requires accounting for the adverse effects due to the mount material and eutectic particles. For instance, in local neighborhoods that contain the mount material, the fourfold symmetry would be extremely low for a dendrite core near the boundary. Therefore, the mount material needs to be accounted for in the symmetry filter. Moreover, the eutectic particles can decrease the fourfold symmetry parameter in a similar way to the mount material. In prior work [11], the mount material and eutectic particles were segmented for sixteen 6 mm \times 6 mm successive serial images spaced \sim 10 μm apart. The location of this region is shown in Figure 1 by a red box. One of these images is used to show the result of accounting for the mount material and eutectic particles in the fourfold symmetry filter.

Figure 4 shows the original image with superimposed segmented dendrite cores in red. The same process outlined schematically in Figure 2 was applied to the original intensity image. To account for the mount material and eutectic particles, there are a few differences from that shown in Figure 2. First, the average image in Figure 2g is modified so that it only reflects the average pixel intensities in areas of the rotated images with an

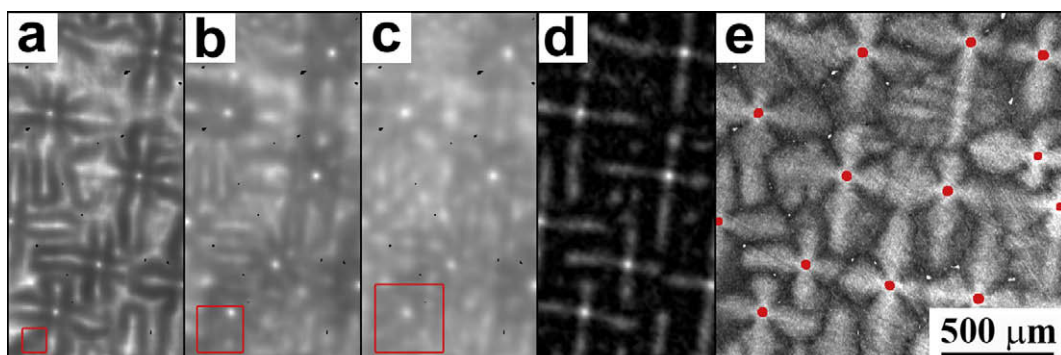


Figure 3. The fourfold symmetry filter was applied to the blue image in Figure 1 using neighborhood sizes of (a) 100 μm , (b) 200 μm and (c) 300 μm . The multiscale image incorporates this information (d) and the dendrite core locations are then segmented and shown in red on the original intensity image (e). (For interpretation of the references to color in this figure legend, the reader is referred to the web version of this paper.)

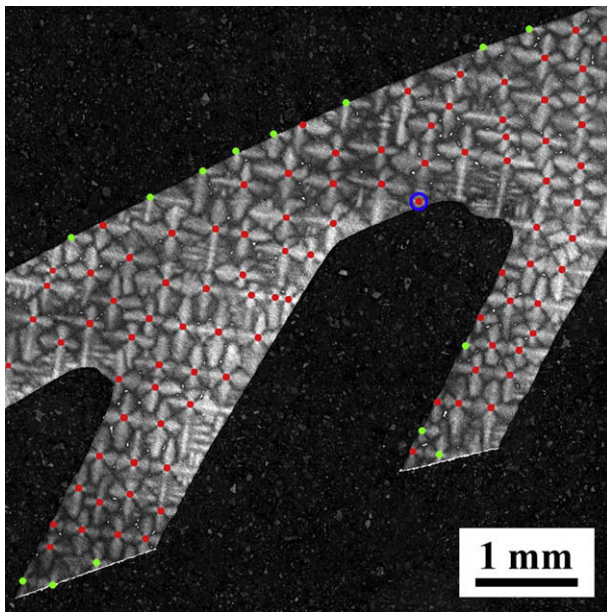


Figure 4. The dendrite cores have been identified (in red) in a 6 mm × 6 mm image taken from a serial slice using the fourfold symmetry filter. The blue circle and green dots refer to incorrectly identified and missed dendrite cores, respectively. (For interpretation of the references to color in this figure legend, the reader is referred to the web version of this paper.)

absence of the mount material and eutectic particles. Second, the fourfold symmetry parameter obtained from the difference image (Fig. 2h) is only summed over pixels that do not belong to the mount material or eutectic particles. Finally, mount material or eutectic particle pixels are given a fourfold symmetry parameter of zero. Again, Figure 4 shows the original intensity image with the dendrite cores identified using a threshold parameter (the red dots have been enlarged slightly to show the dendrite core locations).

To assess the quality of this technique, the results of the automated symmetry-based technique were compared to true results obtained from manual identification of the dendrite cores. The symmetry-based technique correctly identified 93 dendrite core locations in this image with only one area incorrectly identified as a dendrite core (secondary dendrite arm intersecting a tertiary arm near the mount material—circled in blue). Additionally, 14 dendrite cores at the mount material/microstructure boundary were not identified (green dots), but might have been identified manually depending on the operator. These dendrites typically contain only two dendrite arms that intersect close to the boundary (in some cases, outside of the boundary); information from adjacent slices is required for identification. Overall, the results of the symmetry-based technique are good considering the difficulty of accounting for confounding features within the image. As can be observed from Figure 3, this technique does extremely well without these confounding features.

This symmetry-based technique can considerably reduce the amount of time spent manually identifying all dendrite cores within a serial image the size of Figure 1

or larger. However, at this point, this technique still requires some manual intervention. One opportunity is to automate the segmentation of the image in Figures 3d and 4, eliminating all user intervention. Another opportunity for serial images is to incorporate information from adjacent slices to augment the extraction of dendrite core locations. A continuity rule may be added for both missed dendrite cores and incorrectly identified features. For instance, a dendrite core will typically appear on multiple slices. For missed dendrite cores, the adjacent slices may have detected dendrite cores, indicating that the missed dendrite core should probably be included. For incorrectly identified features, the adjacent slices may not have detected dendrite cores, indicating that the incorrectly identified feature is not a dendrite core. These are left for future work, but are essential for fully automating this process to construct the 3-D dendrite core structure.

In summary, an automated image processing technique for extracting symmetric features in microstructural images is discussed (shown schematically in Fig. 2). This technique is then applied to a single crystal Ni-based superalloy to identify dendrite core locations by using their fourfold symmetry as viewed along the $\langle 1\ 0\ 0 \rangle$ growth direction. Overall, the results of this symmetry-based technique are good (cf. Figs. 3e and 4) and the amount of manual intervention is much less than the manual identification of all dendrite core locations. The significance of this work is that techniques such as this will be instrumental for microstructural characterization of materials as the amount of imaging information continues to increase.

This work was performed at the Air Force Research Laboratory, Materials and Manufacturing Directorate, AFRL/RXLM, Wright-Patterson Air Force Base, OH.

- [1] M.D. Uchic, M.A. Groeber, D.M. Dimiduk, J.P. Simmons, *Scripta Materialia* 55 (2006) 23.
- [2] M.A. Groeber, B.K. Haley, M.D. Uchic, D.M. Dimiduk, S. Ghosh, *Materials Characterization* 57 (2006) 259.
- [3] M.A. Groeber, S. Ghosh, M.D. Uchic, D.M. Dimiduk, *Acta Materialia* 56 (2008) 1257.
- [4] M.D. Uchic, M. De Graef, R. Wheeler, D.M. Dimiduk, *Ultramicroscopy* 109 (2009) 1229.
- [5] J.P. Simmons, P. Chuang, M.L. Comer, M. Uchic, J.E. Spowart, M. De Graef, *MSMSE* 17 (2009) 025002.
- [6] E.B. Gulsoy, M. De Graef, *Microscopy & MicroAnalysis* 15 (S2) (2009) 606CD.
- [7] E.B. Gulsoy, J.P. Simmons, M. De Graef, *Scripta Materialia* 60 (2009) 381.
- [8] D.J. Rowenhorst, A. Gupta, C.R. Feng, G. Spanos, *Scripta Materialia* 55 (2006) 11.
- [9] A.C. Lewis, J.F. Bingert, D.J. Rowenhorst, A. Gupta, A.B. Geltmacher, G. Spanos, *MSE A* 418 (2006) 11.
- [10] J. Madison, J.E. Spowart, D.J. Rowenhorst, J. Fiedler, T.M. Pollock, In *Superalloys* (2008) 881.
- [11] M.A. Tschopp, M.A. Groeber, R. Fahringer, J.P. Simmons, A.H. Rosenberger, C. Woodward, *MSMSE*, submitted for publication.